ATF3-induced activation of the NF-κB pathway results in acquired PARP inhibitor resistance in pancreatic adenocarcinoma

Yang Liu
Department of General Surgery, Pancreatic Disease Center, Ruijin Hospital, Shanghai Jiaotong University School of Medicine

Yizhi Cao
Department of General Surgery, Pancreatic Disease Center, Ruijin Hospital, Shanghai Jiaotong University School of Medicine

Pengyi Liu
Department of General Surgery, Pancreatic Disease Center, Ruijin Hospital, Shanghai Jiaotong University School of Medicine

Shuyu Zhai
Department of General Surgery, Pancreatic Disease Center, Ruijin Hospital, Shanghai Jiaotong University School of Medicine

Yihao Liu
Department of General Surgery, Pancreatic Disease Center, Ruijin Hospital, Shanghai Jiaotong University School of Medicine

Xiaomei Tang
Department of General Surgery, Pancreatic Disease Center, Ruijin Hospital, Shanghai Jiaotong University School of Medicine

Jiayu Lin
Department of General Surgery, Pancreatic Disease Center, Ruijin Hospital, Shanghai Jiaotong University School of Medicine

Minmin Shi
Department of General Surgery, Pancreatic Disease Center, Ruijin Hospital, Shanghai Jiaotong University School of Medicine

Debin Qi
Department of General Surgery, Pancreatic Disease Center, Ruijin Hospital, Shanghai Jiaotong University School of Medicine

Xiaxing Deng
Department of General Surgery, Pancreatic Disease Center, Ruijin Hospital, Shanghai Jiaotong University School of Medicine

Youwei Zhu

Department of General Surgery, Pancreatic Disease Center, Ruijin Hospital, Shanghai Jiaotong University School of Medicine

Weishen Wang

Department of General Surgery, Pancreatic Disease Center, Ruijin Hospital, Shanghai Jiaotong University School of Medicine

Baiyong Shen (shenby@shsmu.edu.cn)

Department of General Surgery, Pancreatic Disease Center, Ruijin Hospital, Shanghai Jiaotong University School of Medicine

---

Research Article

Keywords: Olaparib, ATF3, NF-κB, Pancreatic cancer

Posted Date: July 25th, 2023

DOI: https://doi.org/10.21203/rs.3.rs-3172142/v1

Additional Declarations: No competing interests reported.

Version of Record: A version of this preprint was published at Cellular Oncology on December 15th, 2023. See the published version at https://doi.org/10.1007/s13402-023-00907-5.

Abstract

Purpose

Olaparib, an inhibitor of poly-(adenosine diphosphate-ribose) polymerase (PARP), has been shown to have anticancer benefits in patients with pancreatic cancer who have a germline mutation in BRCA1/2. However, resistance acquired on long-term exposure to olaparib significantly impedes clinical efficacy.

Methods

In this study, the chromatin accessibility and differentially expressed transcripts of parental and olaparib-resistant pancreatic cancer cell lines were assessed using the Assay for Transposase Accessible Chromatin with sequencing (ATAC-seq) and mRNA-seq. Detection of downstream genes regulated by transcription factors using ChIP (Chromatin immunoprecipitation assay).

Results

According to pathway enrichment analysis, differentially expressed genes in olaparib-resistant cells were remarkably enriched in the NF-κB signaling pathway. With ATAC-seq, we identified chromatin regions with higher accessibility in olaparib-resistant cells and predicted a series of important transcription factors. Among them, activating transcription factor 3 (ATF3) was significantly highly expressed. Functional experiments verified that inhibition of ATF3 suppressed the NF-κB pathway significantly and restored olaparib sensitivity in olaparib-resistant cells.

Conclusion

Experiments in vitro and in vivo indicate ATF3 enhances olaparib resistance through the NF-κB signaling pathway, suggesting that ATF3 could be employed as an olaparib sensitivity and prognostic indicator in patients with pancreatic cancer.

Introduction

Pancreatic ductal adenocarcinoma (PDAC) is an extremely malignant solid tumor with a dismal prognosis and a meager 10% 5-year survival rate.[1] Surgery and adjuvant chemotherapy are the standard therapeutic approaches for pancreatic cancer.[2] However, because of the absence of screening indicators and early metastases, only 10–15% of pancreatic cancer patients access radical surgery.[3] For 4–7% of pancreatic cancer patients with BRCA germline mutations, olaparib can be used as a maintenance therapy.[4] Yet, severe olaparib resistance is a significant contributing factor to treatment failure. It is thus crucial to clarify the mechanisms of olaparib resistance in PDAC.

Olaparib is an inhibitor of poly-ADP ribose polymerase (PARP) authorized as a maintenance treatment for patients with BRCA1/2 mutations. PARP1 and PARP2 are involved in regulating the base excision repair pathway, which is essential for repairing single-strand breaks (SSBs). BRCA1 and BRCA2 are critical regulators of homologous recombination (HR), an important pathway for repairing double-stranded DNA damage (DSBs).[5] PARPi hinders the repair of SSBs, leading to the generation of DSBs in replicating cells, which are repaired by non-homologous end joining or HR. Because non-homologous end joining is more error-prone and generates chromosomal aberrations, tumor cells deficient in BRCA1 or BRCA2 are more susceptible to PARPi via the synthetic lethality mechanism.[6]

Olaparib has been found in clinical trials to be effective in patients with BRCA1/2-deficient breast or ovarian cancer.[7, 8] Furthermore, a recent study shows that maintenance with olaparib improves progression-free survival in PDAC patients with germline BRCA mutations.[9] Like the majority of chemotherapeutic agents, resistance to olaparib is prevalent in the clinical setting. Although studies on BRCA-mutated cell lines for breast and ovarian cancer have revealed mechanisms of resistance to olaparib, there have been few studies in pancreatic cancer.[10] It is thus urgent to explore mechanisms underlying olaparib resistance in pancreatic cancer.

Activated transcription factor (ATF) belongs to the ATF/cyclic AMP response element-binding (ATF/CREB) protein family, a group of basic leucine zipper (bZIP) transcription factors.[11] ATF3 exercises transcriptional repression or activation by forming homo- or heterodimers with other proteins possessing a bZIP structural domain, such as C/EBP, AP-1, and members of the Maf protein family.[12] As a stress-response factor, ATF3 takes a significant part in the control of glucose homeostasis, the metabolism of lipids, and immunological responses.[13, 14] Recent studies have shown that deletion of ATF3 can prevent KRAS-mediated pancreatic cancer.[15] while other studies have demonstrated that ATF3 enhances chemotherapeutic drug resistance in breast cancer and chronic myelogenous leukemia by a variety of mechanisms.[16, 17]

In this study, we aimed to induce olaparib resistance in the Capan-1 parental cells to investigate its mechanisms in PDAC. Capan-1 is a BRCA2-deficient cell line that is highly susceptible to PARP inhibitors.[18] We aimed to screen for genes relevant to olaparib resistance with the combined use of Assay for Transposase Accessible Chromatin with sequencing (ATAC-seq) and mRNA-seq analysis in the hope of identifying pathways in olaparib resistance and finding ways of restoring olaparib sensitivity.

Methods

Cell culture and reagents

Capan-1 cell line and capan-1 resistant cells were generously gifted by the State Key Laboratory of Drug Research, Shanghai Institute of Materia Medica, Chinese Academy of Sciences (Shanghai, China). Capan-1 cells were cultured in IMDM (BIOAGRIO, Shanghai, China) with 10% fetal bovine serum and 1%

penicillin/streptomycin. Construction of olaparib-resistant capan-1 cells by repeated treatment of capan-1 parental cells with gradually increasing olaparib concentrations.(19) All cells were cultured in an incubator containing 5% CO_2 at 37 ℃, and the culture was free of contamination.

Small interfering RNA transfection

ATF3 small interfering RNA (si-ATF3) and negative control siRNA (si-NC) were synthesized by BioeGene (Shanghai, China). The cells were inoculated into 6-well plates, and cell status was observed and transfected after 24 hours. Transfections were performed using Lipofectamine 3000 (Invitrogen, Waltham, MA), with a final siRNA concentration of 50 nM. Cells were collected 48 h after transfection for further processing. siRNA sequences are listed in Supplementary Table S1.

Western blotting

To extract total protein, cells were lysed on ice with RIPA buffer (Solarbio, Beijing, China) containing 1% protease and phosphatase inhibitors. After centrifugation at 12,000 rpm for 15 minutes, the supernatant was extracted and the protein concentration was measured with bicinchoninic acid (Thermo Fisher Scientific, Waltham, MA), and then added to 5x protein loading buffer and boiled at 100°C for 15 min. Samples were loaded and separated on 12.5% SDS-PAGE gels (EpiZyme, Shanghai, China) and transferred to polyvinylidene fluoride membranes. After blocking with 5% skim milk powder, the membrane was incubated with primary antibody at 4 ℃ overnight. The following primary antibodies were used: anti-ATF3 (A13469, ABclonal, Wuhan, China), anti-P65 (#8242, CST, Danvers, MA), anti-p-p65 (#3033, CST, Danvers, MA), and anti-ACTB (81115-1-RR, Proteintech, Rosemont, IL). β-actin (ACTB) was used as the control. Subsequent incubation with the corresponding secondary antibody for 2 h was followed by luminescence.

RNA extraction and quantitative real-time PCR (qRT-PCR)

To extract total RNA from cells, we used SteadyPure Quick RNA Extraction Kit (AG21023, Accurate Biology, Hunan, China) following the manufacturer's instructions, and the concentration was determined. cDNA was generated using an Evo M-MLV RT Kit II (AG11711, Accurate Biology) for reverse transcription. qRT-PCR used a SYBR Green I chimeric fluorescence assay (AG11739, Accurate Biology). The primer sequences are listed in Supplementary Table S2.

Cell migration assays

In the lowest chamber of a 24-well Transwell plate (Costar Corning, Cambridge, MA), IMDM that was supplemented with 10% FBS was introduced. After being resuspended in media devoid of serum, 5×10^4 cells were loaded to the top chamber. Following incubation for 24 hours, the cells were stained with crystal violet at a concentration of 0.1% for 10 minutes before being fixed with 4% paraformaldehyde for 20 minutes. Using a microscope, an assessment was made of the average amount of invading cells over five different fields of view.

Cell Counting Kit-8 (CCK-8) assay

The CCK-8 test was employed to assess the viability of the cells (Dojindo, Kumamoto, Japan). In order to prepare the cells for drug treatment, 3×10^3 of them were seeded onto 96-well plates and cultivated for 48 hours. This was then followed by a 72-hour pharmacological therapy. After adding 10 μL of CCK-8 test reagent and 90 μL medium and allowing the mixture to incubate for two hours, the absorbance was determined by utilizing a BioTek Gen5 system and measuring it at 450 nm.

Colony formation assay

Inoculate six-well plate with 1.5×10^3 cells per well. The culture was continued for 10 days followed by siRNA transfection and 24 hours later treated with different approaches. After treatment, the cells were rinsed with PBS and fixed with 4% paraformaldehyde. Finally stained with crystal violet for 10 minutes and photographed.

Chromatin immunoprecipitation (ChIP)

To detect binding of transcription factors to specific genomic regions, ChIP-Seq and ChIP-qPCR assays were carried out. Cells were quenched with glycine for 10 minutes after being crosslinked using 1% formaldehyde for 10 minutes. Cross-linked chromatin was ultrasonically cleaved into 200–500 bp fragments. Anti-ATF3 antibody (ab254268, Abcam, Cambridge, UK) and IgG antibody were used for immune binding and immunoprecipitation. Cross-linking and DNA purification were then carried out. A Hieff NGS MaxUp II DNA Library Prep Kit for Illumina (Yeasen, Shanghai, China) was used to construct the library for ChIP-Seq. Sequencing was performed on a NovaSeq 6000 system using the NovaSeq 6000 S4 Reagent Kit v1.5 (Illumina, San Diego, CA). For ChIP-qPCR, purified DNA fragments were analyzed by quantitative real-time PCR using specific ChIP-qPCR primers. ChIP-qPCR primers are listed in Supplementary Table S3.

Flow cytometric analysis

To assess apoptosis following drug treatment, floating and adherent cells were collected, washed, resuspended in binding buffer, and double-stained with an Annexin V-FITC/PI Apoptosis Detection Kit (A211-01, Vazyme, Nanjing, China). After a 15-minute incubation period at room temperature and without light, cells were examined by flow cytometry within an hour.

Mouse tumor model

Five-week-old male BALB/C nude mice were purchased from the Chinese Academy of Sciences (Shanghai, China). Capan-1-OR cells (6×10^5 cells/locus) were washed, resuspended in PBS, and injected subcutaneously into randomly grouped mice to establish a subcutaneous tumor model. Every three days starting from day 5, the length (a) and width (b) of the tumor were gauged, and the tumor volume was calculated using the formula $(a \times b^2)/2$. Mice were killed 26 days after injection.

mRNA sequencing

Following extraction of RNA from cells, an RNA library was constructed using 1 μg total RNA and a VVAHTS Universal V8 RNA-seq Library Prep Kit for Illumina (Cat. NR605-0, Vazyme, Nanjing, China).

Purification and enrichment of PCR products were performed, and a Qubit 2.0 fluorometer (Invitrogen, Carlsbad, CA) was utilized for library quantification. The NovaSeq 6000 S4 Reagent Kit v1.5 was employed for the sequencing process, which was carried out on a NovaSeq 6000 high-throughput sequencer (Illumina, San Diego, CA). We defined P value < 0.05, absolute value of fold change > 1.5 as differential expressed genes (DEGs)

Assay for Transposase Accessible Chromatin with sequencing

Centrifuging cells at 500 g for 5 min to collect them, resuspending them in lysis buffer that had already been chilled, and placing them on ice for 10 min. After centrifuging cells at 500 g for 5 min at 4 degrees Celsius in order to extract the nuclei, an ATAC library was produced with the use of a TruePrep DNA Library Prep Kit V2 for Illumina (TD501, Vazyme, Nanjing, China) in accordance with the guidelines provided by the manufacturer. Transposable DNA fragments were isolated, purified, and enriched using 15 cycles of PCR amplification. The VAHTS DNA Clean Beads were employed for the purification of PCR products, and a Qubit 2.0 fluorometer (Invitrogen, Carlsbad, CA) was utilized for the quantification of library samples. The ATAC-seq library was end-pair-sequenced on the Novaseq 6000 platform.

Statistical analysis

The graphing and statistical work was done in GraphPad Prism 8. At least three duplicates of each experiment were conducted, and the data were statistically summarized as the mean ± standard deviation (SD). Means were compared using the unpaired Student's t-test to determine significance. The threshold for significance was determined to be $P < 0.05$.

Results

Functional and pathway enrichment analyses of genes associated with acquired olaparib resistance

We used olaparib-resistant Capan-1 cells (Capan-1-OR cells) to investigate mechanisms of olaparib resistance. The half-maximal inhibitory concentration (IC50) value of olaparib in parental Capan-1 cells was 3.355 μM, while for Capan-1-OR cells, the IC50 value was 69.77 μM, far exceeding that of parental Capan-1 cells(Fig. 1A), demonstrating a greater degree of Olaparib resistance in established resistant cells than in the parental cells. The percentage of both early and late apoptotic cells dramatically increased on olaparib treatment of parental Capan-1 cells, but the level of apoptosis in Capan-1-OR cells was unaffected by olaparib treatment (Fig. 1B-C). To identify genes potentially involved in olaparib resistance in Capan-1-OR cells, RNA sequencing was carried out using three biological replicates for each sample. There were 6043 differentially expressed genes (DEGs) were identified, comprising 3765 genes with upregulated expression and 3793 genes with downregulated expression (Fig. 1D-F). To uncover key pathways, Kyoto Encyclopedia of Genes and Genomes (KEGG) and Gene Set Enrichment Analysis (GSEA)

analyses were employed. We found that DEGs in olaparib-resistant cells were primarily enriched in the NF-kappa B signaling pathways (Fig. 1. G-H).

ATF3 motif is highly enriched in the specific open chromatin of olaparib-resistant cells

Recent researches have demonstrated the significance of epigenetic modifications in drug resistance, especially changes in chromatin accessibility. We hypothesized that chromatin accessibility contributes to resistance to olaparib. We used ATAC-seq to evaluate changes in chromatin accessibility between parental Capan-1 cells and Capan-1-OR cells. The ATAC-seq data had a coordinate distribution of fragment insert sizes of approximately 200 bp, indicating that the data were of high quality (Fig. S1A). We used differentially accessible peak analysis to investigate differences in chromatin accessibility between the two cell lines. Compared to parental cells, Capan-1-OR cells had more accessibility in 142 regions, while 1420 regions in chromatin were less accessible in Capan-1-OR cells; we term these locations "hyper" and "hypo", respectively (Fig. 2A). Transcription factors (TFs) bind to motifs in enhancers and promoters of their target genes and require an open chromatin conformation to control the expression of genes. We evaluated putative TFs present in the DARs of Capan-1-OR cells using the motif-finding program HOMER (Fig. 2B). When TFs bind to their corresponding motifs, this may cause nucleosome eviction and generation of open chromatin sites. We aimed to predict TF binding and chromosomal occupation by combining ATAC-seq chromatin accessibility data with existing TF motif information. TF motif occurrence and binding sites were examined in DARs in flanking sequences of 200 bp surrounding the ATAC-seq peaks.

We ranked the top 10 TF candidates in Capan-1-OR cells according to their enrichment in hyper-accessible areas and examined the mRNA levels of these TFs in Capan-1-OR and Capan-1 cells to better understand their regulation (Fig. 2B). In Capan-1-OR cells, ATF3 levels were considerably elevated. Western blotting confirmed the elevation of ATF3 and phosphorylated NF-κB at the protein level in Capan-1-OR cells (Fig. 2C). In addition, we found that ATF3 expression was higher in tumor than in normal tissues in the TCGA-PAAD database (Fig. 2D).

Olaparib-resistant PDAC cells with a silenced ATF3 regain olaparib sensitivity and reduce malignancy in Vitro

We used small interfering RNA transfection to suppress ATF3 expression to determine the function of ATF3 in olaparib-resistant PDAC cells (Fig. 3A). Examining the olaparib IC50 values in control and ATF3-knockdown Capan-1-OR cells, we found that IC50 values were much lower when ATF3 was silenced (Fig. 3B). Meanwhile, colony formation assays revealed that the number of colonies in Capan-1 OR cells under olaparib treatment was significantly reduced after ATF3 knockdown (Fig. 3C-D). These results suggest that high ATF3 levels impart olaparib resistance in PDAC. At the same time, we found that the silencing of ATF3 can reduce the protein expression of p-p65 and the transcription level of some essential regulatory genes in the NF-κB signaling pathway (Fig. 3A, E). This indicates that ATF3 may function in

olaparib-resistant cells by regulating the NF-κB signaling pathway. Furthermore, ATF3 silencing greatly diminished the migration of olaparib-resistant cells in transwell assays, which indicates that ATF3 may promote the invasiveness of olaparib-resistant pancreatic cancer (Fig. 3F). The percentages of both early and late apoptotic cells increased substantially with Olaparib treatment after ATF3 interference, suggesting an important role for ATF3 in maintaining cell survival in Capan-1-OR cells exposed to olaparib (Fig. 3G-H). Overall, the data demonstrate that higher expression of ATF3 increases resistance to Olaparib in pancreatic cancer cells and confers greater malignancy in Capan-1-OR cells as compared with parental cells.

ATF3 regulates active histone modifications to affect downstream targets via activation of the NF-κB signaling pathway

To further investigate the manner by which ATF3 affects specific downstream targets, we used chromatin immunoprecipitation with next-generation sequencing (ChIP-seq), revealing that ATF3 silencing decreased overall H3K27 acetylation (H3K27ac) marking active enhancers (Fig. 4A-B) and H3K4 trimethylation (H3K4me3) marking active promoters (Fig. 4C-D). As shown in Fig. 4E–H and Fig. S2A-B, ATF3 directly binds to the promoter loci of key genes involved in NF-κB signaling regulation, including TRAF1, BIRC3 and ICAM1, followed by changes to the H3K27ac- and H3K4me3-enriched regions in Capan-1-OR cells compared with that in parent cells. Our findings show that ATF3 maintains olaparib resistance in Capan-1 cells by binding to the transcription starting site (TSS) of important genes in NF-κB signaling pathways, causing alterations in their chromatin accessibility and histone modification.

The NF-κB inhibitor parthenolide could be used in combination with olaparib to restore its sensitivity in resistant PDAC cells

If ATF3 promotes olaparib resistance in PDAC by stimulating the NF-κB signaling pathway, then targeting the NF-κB pathway may be a viable method for overcoming Olaparib resistance. The NF-κB signaling pathway was pharmacologically disrupted by using NF-κB inhibitor parthenolide. We first predicted the drug sensitivity of TCGA database samples to parthenolide based on the Genomics of Drug Sensitivity in Cancer (GDSC) database and found that the cohort with higher ATF3 expression had lower IC50 values (Fig. 5A). Parthenolide administration to OR cells dramatically suppressed p-p65 expression, as evidenced by western blotting (Fig. 5B). Using flow cytometry, we then determined the proportion of apoptotic cells after treating OR cells with olaparib and parthenolide separately or in conjunction. The results showed that the extent of apoptosis in the olaparib single-agent group did not significantly differ from that in the control group, while the extent of apoptosis in the parthenolide group was 37.00%. (Fig. 5C-D). The extent of apoptosis increased to 63.64% in the olaparib + parthenolide group. Our findings indicate that parthenolide re-sensitizes olaparib-resistant cells to olaparib and provide further evidence that through stimulating the NF-κB signaling pathway, ATF3 enhances olaparib resistance in PDAC.

We constructed a mouse subcutaneous tumor model employing olaparib-resistant cells to investigate the medication combination's anticancer efficacy in vivo. The mice were treated with saline or with olaparib

(20 mg/kg, IP) and parthenolide (10 mg/kg, IP) alone or in combination. All drugs were administered once daily via intraperitoneal injection. The olaparib + parthenolide group showed a greater anti-tumor effect at the end of treatment compared to olaparib or parthenolide monotherapy (Fig. 5E-G). The olaparib monotherapy group exhibited no prominent antitumor efficacy when compared to the control group, whereas the combination of olaparib and parthenolide had the best anticancer effect among the four groups. The in vitro findings are consistent with the in vivo findings, indicating that blocking the NF-κB signaling pathway could be an effective therapeutic strategy for reversing olaparib resistance in PDAC. In conclusion, we presented a potential combined medication approach for patients with PDAC and BRAC mutations.

Discussion

Resistance to olaparib is a significant concern in the therapy of BRCA-mutated PDAC. Current resistance mechanisms proposed for olaparib include DNA replication fork protection, homologous recombination repair restoration, reverse mutagenesis, recovery of ADP-ribosylation, and epigenetic modifications.[10, 18, 20, 21] It has been shown that epigenetic modifications play a significant role in PARPi resistance. However, most studies have concentrated on breast and ovarian malignancies. To clarify the mechanism of olaparib resistance in pancreatic cancer, we used olaparib-resistant Capan-1 cells in vitro. We conducted mRNA-seq and ATAC-seq analyses on olaparib-resistant and parental cells to identify transcriptional and epigenetic landscape alterations for tumor cells in the resistant state. By chromatin accessibility analysis, we identified ATF3 as a key transcription factor for PDAC resistance to olaparib.

ATF3 has been shown to be expressed in a range of malignancies; however, its effects may be different in different cancer types.[11] Overexpression of ATF3 has been shown to dramatically enhance the metastatic potential of prostate cancer.[22] In breast cancer, ATF3 increases tumor invasion and metastasis by activating CCNA1 and MMP13.[23] There is evidence that ATF3 is implicated in increased paclitaxel resistance in breast cancer.[24] Similarly, elevated ATF3 expression promotes radioresistance in breast cancer cells.[25] In contrast, increased ATF3 expression renders cisplatin-resistant gastric cancer cells susceptible to cisplatin.(26) Further, ATF3 induces apoptosis in prostate, colon, and lung malignancies.[27, 28] In pancreatic cancer, ATF3 is essential for the progression and maintenance of high-grade PanIN and PDAC and has been identified as a critical gene for perineural invasion of PDAC.[15, 29] A recent study found that lncRNA-MTA2TR increases MTA2 expression by recruiting ATF3 to the MTA2 promoter region, enhancing the invasion and proliferation capacities of PDAC.[30] Thus, the involvement of ATF3 in tumor growth, metastasis, and treatment resistance varies with tumor type. In pancreatic cancer, ATF3 appears to play a more oncogenic role, consistent with our results.

In our study, we analyzed the chromatin accessibility of genome-wide profiles by ATAC-seq and screened ATF3 as a key transcription factor for PDAC resistance to olaparib. In olaparib-resistant cells, we observed a rise in ATF3 protein expression. When we suppressed ATF3 expression in olaparib-resistant cells, the IC50 for olaparib treatment decreased substantially, and the rate of apoptosis increased. In addition,

suppression of ATF3 expression diminished the invasive potential of olaparib-resistant cells. These findings support the hypothesis that ATF3 induces acquired resistance in PDAC to olaparib.

We further investigated the mechanism by which ATF3 induces olaparib resistance in pancreatic cancer. ATF3 expression is induced by multiple stress-related signals and implicates several intracellular signaling pathways, such as the Smad, NF-κB, c-Myc, JNK, ERK, p53, and p38 pathways.[31–35] Our enrichment analysis revealed high enrichment of the NF-κB pathway in olaparib-resistant cells. NF-κB transcription factors play important roles in immunity, stress responses, apoptosis and differentiation, and participate in tumor cell proliferation, metastasis, angiogenesis and therapeutic resistance.[36, 37] Recent research has demonstrated that the NF-κB pathway promotes gemcitabine resistance in PDAC.[38] Several studies have reported mutual regulation of ATF3 and NF-κB. It has been found that ATF3 not only blocks p65 from binding to the target promoter by recruiting histone deacetylase 1 (HDAC1) into the transcriptional complex, but also reduces NF-κB activity via directly binding to the p65 subunit.[39] Most current research indicates that ATF3 regulates NF-κB in a predominantly negative manner.[40] However, our investigation showed that reduction of ATF3 in olaparib-resistant cells led to a considerable decrease in p-p65 (activated RelA) levels. The introduction of the NF-κB inhibitor, parthenolide, greatly decreased olaparib resistance in olaparib-resistant cells, and we obtained the same finding in a mouse subcutaneous tumor model. These results led us to conclude that ATF3 induces acquired resistance to olaparib in PDAC by activating the NF-κB signaling pathway.

Taken together, our findings suggest the activation of the NF-κB pathway by ATF3 is crucial for olaparib resistance in PDAC. This study demonstrated that ATF3 may be utilized as a biomarker to assess olaparib sensitivity in PDAC patients and may be a viable target to improve the treatment response to olaparib-resistant PDAC. Meanwhile, we offer a potential targeted strategy to overcome PDAC resistance to Olaparib by the use of NF-κB inhibitors.

Declarations

Acknowledgments: We thank Prof. Zehong Miao from the Division of Anti-Tumor Pharmacology, State Key Laboratory of Drug Research, Shanghai Institute of Materia Medica, Chinese Academy of Sciences for Olaparib-resistance Capan-1 cell line as a kindly gift to us.

Ethical Approval: All animal experiments were approved by the Animal Ethics Committee of Shanghai Jiao Tong University (License number: SYXK Shanghai 2018-0027).

Competing interests: The authors declare no competing interests.

Authors' contributions: Study concept and design, Liu Y, Cao Y, Wang W, Shen B; acquisition of data, Liu Y, Liu P, Zhai S, Lin J, Tang X, Shi M, ; analysis and interpretation of data, Liu Y, Cao Y, Liu Y; drafting of the manuscript, Liu Y, Cao Y; critical revision of the manuscript for important intellectual content, Shen B, Wang W; statistical analysis, Liu Y, Qi D; obtained funding, Shen B, Wang W, Zhu Y, Deng X; administrative,

technical, or material support, Shen B, Wang W, Zhu Y; study supervision, Shen B, Wang W, Zhu Y. All authors read and approved the final manuscript.

Funding: This study was supported by grants from the National Natural Science Foundation of China (Nos.82073326), the Shanghai Sailing Program (No.22YF1426200), the Jiaotong University Medical-Engineering Cross Fund (No. YG2022QN007), the Shenkang center city hospital emerging frontier technology joint research project (No. SHDC12020121), and the Guangci Clinical Technology Sailing Project (No. YW20210033).

Availability of data and materials: Data are available in a public, open-access datasets. ATAC-seq, ChIP-Seq and mRNA-seq data generated in this study are deposited at the National Omics Data Encyclopedia (NODE) with the accession code OEP004144 (https://www.biosino.org/node/).

References

1. Mizrahi JD, Surana R, Valle JW, Shroff RT. Pancreatic cancer. The Lancet. **395**(10242):2008-20. (2020);
2. Neoptolemos JP, Kleeff J, Michl P, Costello E, Greenhalf W, Palmer DH. Therapeutic developments in pancreatic cancer: current and future perspectives. Nat Rev Gastroenterol Hepatol. **15**(6):333-48. (2018);
3. Siegel RL, Miller KD, Fuchs HE, Jemal A. Cancer Statistics, 2021. CA Cancer J Clin. **71**(1):7-33.(2021);
4. Park W, Chawla A, O'Reilly EM. Pancreatic Cancer: A Review. Jama. **326**(9):851-62.(2021);
5. Mateo J, Lord CJ, Serra V, Tutt A, Balmaña J, Castroviejo-Bermejo M, et al. A decade of clinical development of PARP inhibitors in perspective. Ann Oncol. **30**(9):1437-47.(2019);
6. Kaufman B, Shapira-Frommer R, Schmutzler RK, Audeh MW, Friedlander M, Balmaña J, et al. Olaparib monotherapy in patients with advanced cancer and a germline BRCA1/2 mutation. J Clin Oncol. **33**(3):244-50.(2015);
7. Robson M, Im S-A, Senkus E, Xu B, Domchek SM, Masuda N, et al. Olaparib for Metastatic Breast Cancer in Patients with a Germline BRCA Mutation. N Engl J Med. **377**(6):523-33.(2017);
8. Moore K, Colombo N, Scambia G, Kim B-G, Oaknin A, Friedlander M, et al. Maintenance Olaparib in Patients with Newly Diagnosed Advanced Ovarian Cancer. N Engl J Med. **379**(26):2495-505.(2018);
9. Golan T, Hammel P, Reni M, Van Cutsem E, Macarulla T, Hall MJ, et al. Maintenance Olaparib for Germline BRCA-Mutated Metastatic Pancreatic Cancer. N Engl J Med. **381**(4):317-27.(2019);
10. Li H, Liu ZY, Wu N, Chen YC, Cheng Q, Wang J. PARP inhibitor resistance: the underlying mechanisms and clinical implications. Mol Cancer. **19**(1):107.(2020);
11. Thompson MR, Xu D, Williams BRG. ATF3 transcription factor and its emerging roles in immunity and cancer. J Mol Med (Berl). **87**(11):1053-60.(2009);

12. Zhou H, Li N, Yuan Y, Jin Y-G, Guo H, Deng W, et al. Activating transcription factor 3 in cardiovascular diseases: a potential therapeutic target. Basic Research in Cardiology. **113**(5):37.(2018);
13. Ku H-C, Cheng C-F. Master Regulator Activating Transcription Factor 3 (ATF3) in Metabolic Homeostasis and Cancer. Front Endocrinol (Lausanne). **11**:556.(2020);
14. Zmuda EJ, Qi L, Zhu MX, Mirmira RG, Montminy MR, Hai T. The roles of ATF3, an adaptive-response gene, in high-fat-diet-induced diabetes and pancreatic beta-cell dysfunction. Mol Endocrinol. **24**(7):1423-33.(2010);
15. Azizi N, Toma J, Martin M, Khalid MF, Mousavi F, Win PW, et al. Loss of activating transcription factor 3 prevents KRAS-mediated pancreatic cancer. Oncogene. **40**(17):3118-35.(2021);
16. Kuroda J, Yamamoto M, Nagoshi H, Kobayashi T, Sasaki N, Shimura Y, et al. Targeting activating transcription factor 3 by Galectin-9 induces apoptosis and overcomes various types of treatment resistance in chronic myelogenous leukemia. Mol Cancer Res. **8**(7).(2010);
17. Borgoni S, Sofyalı E, Soleimani M, Wilhelm H, Müller-Decker K, Will R, et al. Time-Resolved Profiling Reveals ATF3 as a Novel Mediator of Endocrine Resistance in Breast Cancer. Cancers. **12**(10).(2020);
18. Edwards SL, Brough R, Lord CJ, Natrajan R, Vatcheva R, Levine DA, et al. Resistance to therapy caused by intragenic deletion in BRCA2. Nature. **451**(7182):1111-5.(2008);
19. Guo N, Li MZ, Wang LM, Chen HD, Song SS, Miao ZH, et al. Repeated treatments of Capan-1 cells with PARP1 and Chk1 inhibitors promote drug resistance, migration and invasion. Cancer biology & therapy. **23**(1):69-82.(2022);
20. Johnson SF, Cruz C, Greifenberg AK, Dust S, Stover DG, Chi D, et al. CDK12 Inhibition Reverses De Novo and Acquired PARP Inhibitor Resistance in BRCA Wild-Type and Mutated Models of Triple-Negative Breast Cancer. Cell Rep. **17**(9):2367-81.(2016);
21. Kondrashova O, Topp M, Nesic K, Lieschke E, Ho G-Y, Harrell MI, et al. Methylation of all BRCA1 copies predicts response to the PARP inhibitor rucaparib in ovarian carcinoma. Nat Commun. **9**(1):3970.(2018);
22. Bandyopadhyay S, Wang Y, Zhan R, Pai SK, Watabe M, Iiizumi M, et al. The tumor metastasis suppressor gene Drg-1 down-regulates the expression of activating transcription factor 3 in prostate cancer. Cancer Research. **66**(24):11983-90.(2006);
23. Kwok S, Rittling SR, Partridge NC, Benson CS, Thiyagaraj M, Srinivasan N, et al. Transforming growth factor-β1 regulation of ATF-3 and identification of ATF-3 target genes in breast cancer cells. Journal of Cellular Biochemistry. **108**(2):408-14.(2009);
24. Chang YS, Jalgaonkar SP, Middleton JD, Hai T. Stress-inducible gene Atf3 in the noncancer host cells contributes to chemotherapy-exacerbated breast cancer metastasis. Proceedings of the National Academy of Sciences. **114**(34):E7159-E68.(2017);
25. Zhao W, Sun M, Li S, Chen Z, Geng D. Transcription factor ATF3 mediates the radioresistance of breast cancer. J Cell Mol Med. **22**(10):4664-75.(2018);
26. Fu D, Wang C, Yu L, Yu R. Induction of ferroptosis by ATF3 elevation alleviates cisplatin resistance in gastric cancer by restraining Nrf2/Keap1/xCT signaling. Cellular & molecular biology letters.

26(1):26.(2021);

27. Chüeh AC, Tse JWT, Dickinson M, Ioannidis P, Jenkins L, Togel L, et al. ATF3 Repression of BCL-X Determines Apoptotic Sensitivity to HDAC Inhibitors across Tumor Types. Clin Cancer Res. **23**(18):5573-84.(2017);
28. Jan YH, Tsai HY, Yang CJ, Huang MS, Yang YF, Lai TC, et al. Adenylate kinase-4 is a marker of poor clinical outcomes that promotes metastasis of lung cancer by downregulating the transcription factor ATF3. Cancer Research. **72**(19):5119-29.(2012);
29. Zhu J-H, Yan Q-L, Wang J-W, Chen Y, Ye Q-H, Wang Z-J, et al. The Key Genes for Perineural Invasion in Pancreatic Ductal Adenocarcinoma Identified With Monte-Carlo Feature Selection Method. Front Genet. **11**:554502.(2020);
30. Zeng Z, Xu FY, Zheng H, Cheng P, Chen QY, Ye Z, et al. LncRNA-MTA2TR functions as a promoter in pancreatic cancer via driving deacetylation-dependent accumulation of HIF-1α. Theranostics. **9**(18):5298-314.(2019);
31. Rohini M, Haritha Menon A, Selvamurugan N. Role of activating transcription factor 3 and its interacting proteins under physiological and pathological conditions. International Journal of Biological Macromolecules. **120**:310-7.(2018);
32. Liang Y, Jiang Y, Jin X, Chen P, Heng Y, Cai L, et al. Neddylation inhibition activates the protective autophagy through NF-κB-catalase-ATF3 Axis in human esophageal cancer cells. Cell Commun Signal. **18**(1):72.(2020);
33. Rohini M, Arumugam B, Vairamani M, Selvamurugan N. Stimulation of ATF3 interaction with Smad4 via TGF-β1 for matrix metalloproteinase 13 gene activation in human breast cancer cells. International Journal of Biological Macromolecules. **134**:954-61.(2019);
34. Tamura K, Hua B, Adachi S, Guney I, Kawauchi J, Morioka M, et al. Stress response gene ATF3 is a target of c-myc in serum-induced cell proliferation. EMBO J. **24**(14):2590-601.(2005);
35. Hamdi M, Popeijus HE, Carlotti F, Janssen JM, van der Burgt C, Cornelissen-Steijger P, et al. ATF3 and Fra1 have opposite functions in JNK- and ERK-dependent DNA damage responses. DNA Repair. **7**(3):487-96.(2008);
36. Oeckinghaus A, Hayden MS, Ghosh S. Crosstalk in NF-κB signaling pathways. Nature Immunology. **12**(8):695-708.(2011);
37. Khan H, Ullah H, Castilho PCMF, Gomila AS, D'Onofrio G, Filosa R, et al. Targeting NF-κB signaling pathway in cancer by dietary polyphenols. Crit Rev Food Sci Nutr. **60**(16):2790-800.(2020);
38. Ding J, Li H, Liu Y, Xie Y, Yu J, Sun H, et al. OXCT1 Enhances Gemcitabine Resistance Through NF-κB Pathway in Pancreatic Ductal Adenocarcinoma. Frontiers in oncology. **11**:698302.(2021);
39. Kwon JW, Kwon HK, Shin HJ, Choi YM, Anwar MA, Choi S. Activating transcription factor 3 represses inflammatory responses by binding to the p65 subunit of NF-κB. Sci Rep. **5**:14470.(2015);
40. Gilchrist M, Thorsson V, Li B, Rust AG, Korb M, Kennedy K, et al. Systems biology approaches identify ATF3 as a negative regulator of Toll-like receptor 4. Nature. **441**(7090):173-8.(2006);

Figures

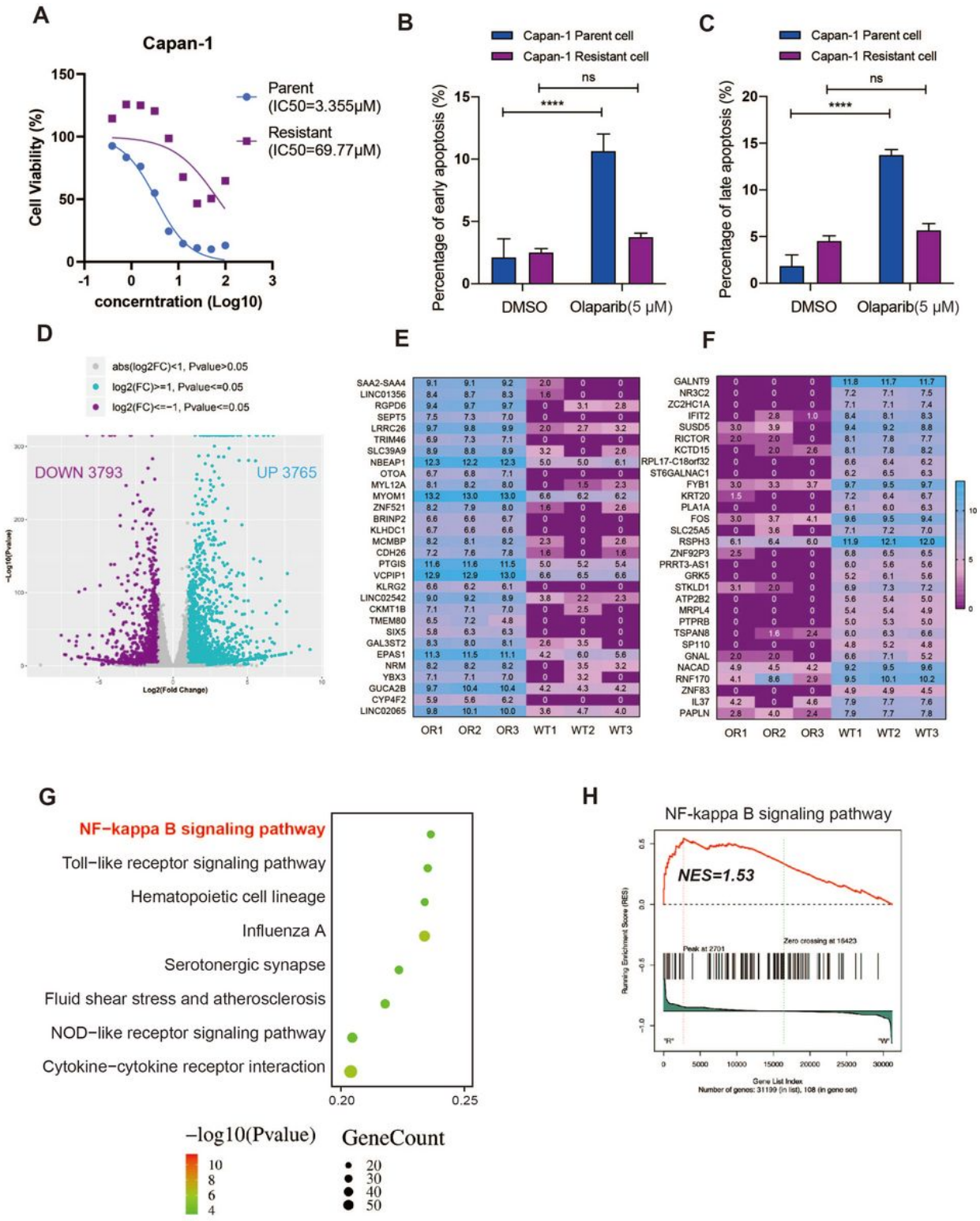

Figure 1

Enrichment analysis of differentially expressed genes (DEGs) in Capan-1-OR cells. (A) Cell viability evaluated using the CCK-8 assay following administration of different concentrations of olaparib to Capan-1 parental cells and Capan-1-OR cells for 72 h. (B-C) Flow cytometric evaluation of apoptosis after

treatment of Capan-1 parental cells and Capan-1-OR cells with olaparib (5 μM) for 72 h. Annexin V-positive cells were deemed to be apoptotic (n=3; NS: not significant; $^{****}P < 0.0001$). (D) Volcano plot of DEGs for Capan-1 parental cells as compared to Capan-1-OR cells. (E-F) Heatmap of gene expression values comparing Capan-1 parental cells and Capan-1-OR cells. (G) Kyoto Encyclopedia of Genes and Genomes (KEGG) pathway analysis for significantly enriched pathways in DEGs. (H) Genomic enrichment analysis (GSEA) of the most enriched pathways of upregulated genes.

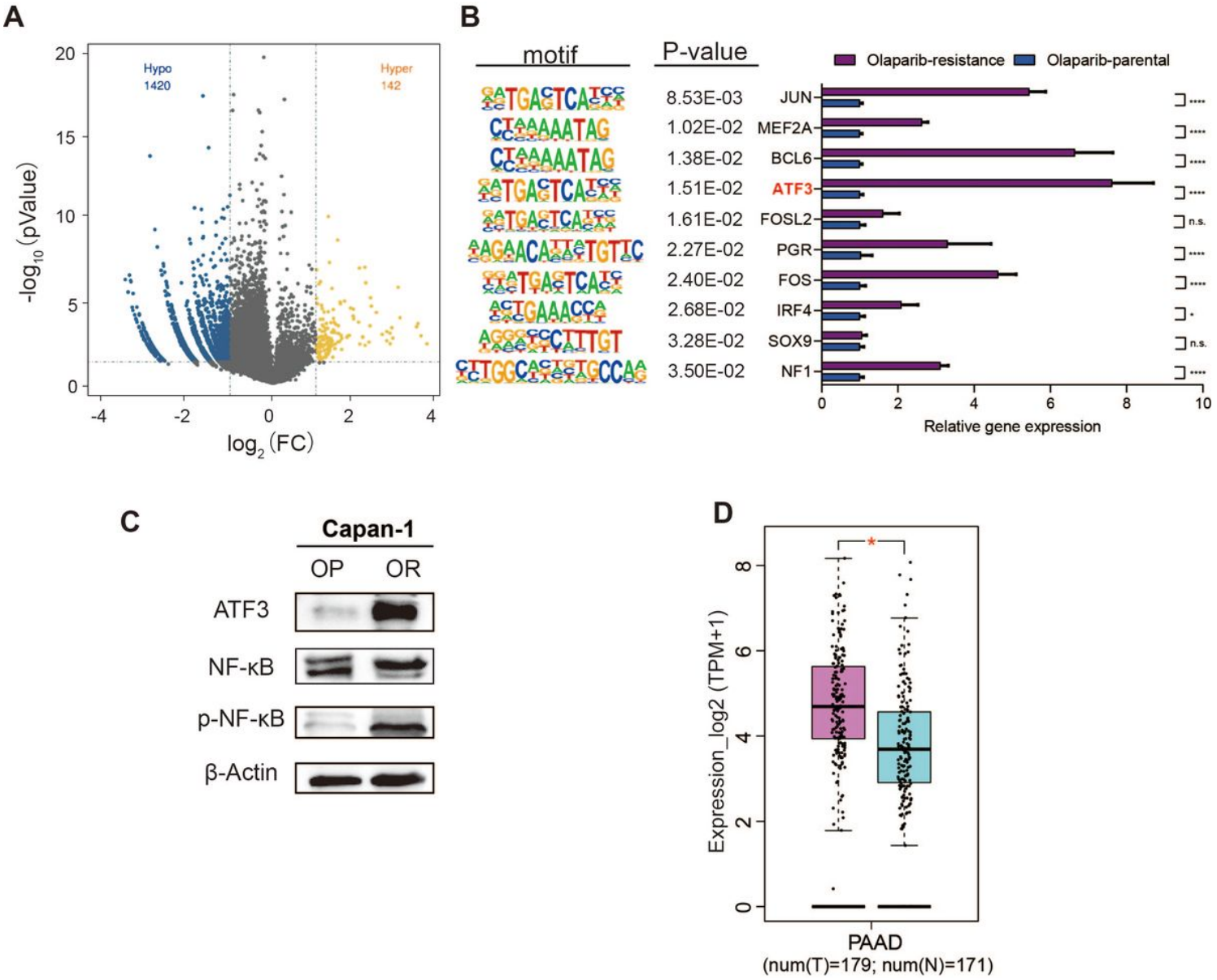

Figure 2

Identification of ATF3 using combined analysis of DARs and DEGs. (A) Volcano plot illustrating differentially accessible regions (DARs) for Capan-1-OR cells as compared with Capan-1 parental cells. (B) Real-time quantitative PCR for mRNA expression of the top ten transcription factors in Capan-1 parental and Capan-1-OR cells. (C) Western blotting showing expression of ATF3, p65 and p-p65 protein in Capan-1 parental cells and Capan-1-OR cells. (D) Box plot showing ATF3 expression in PDAC and

normal tissues. Results were obtained using a combined analysis of the TCGA (PAAD) and GETx databases. (E) Relationship between ATF3 expression and overall survival of PDAC patients based on Kaplan-Meier analysis using the Ruijin-PDAC database.

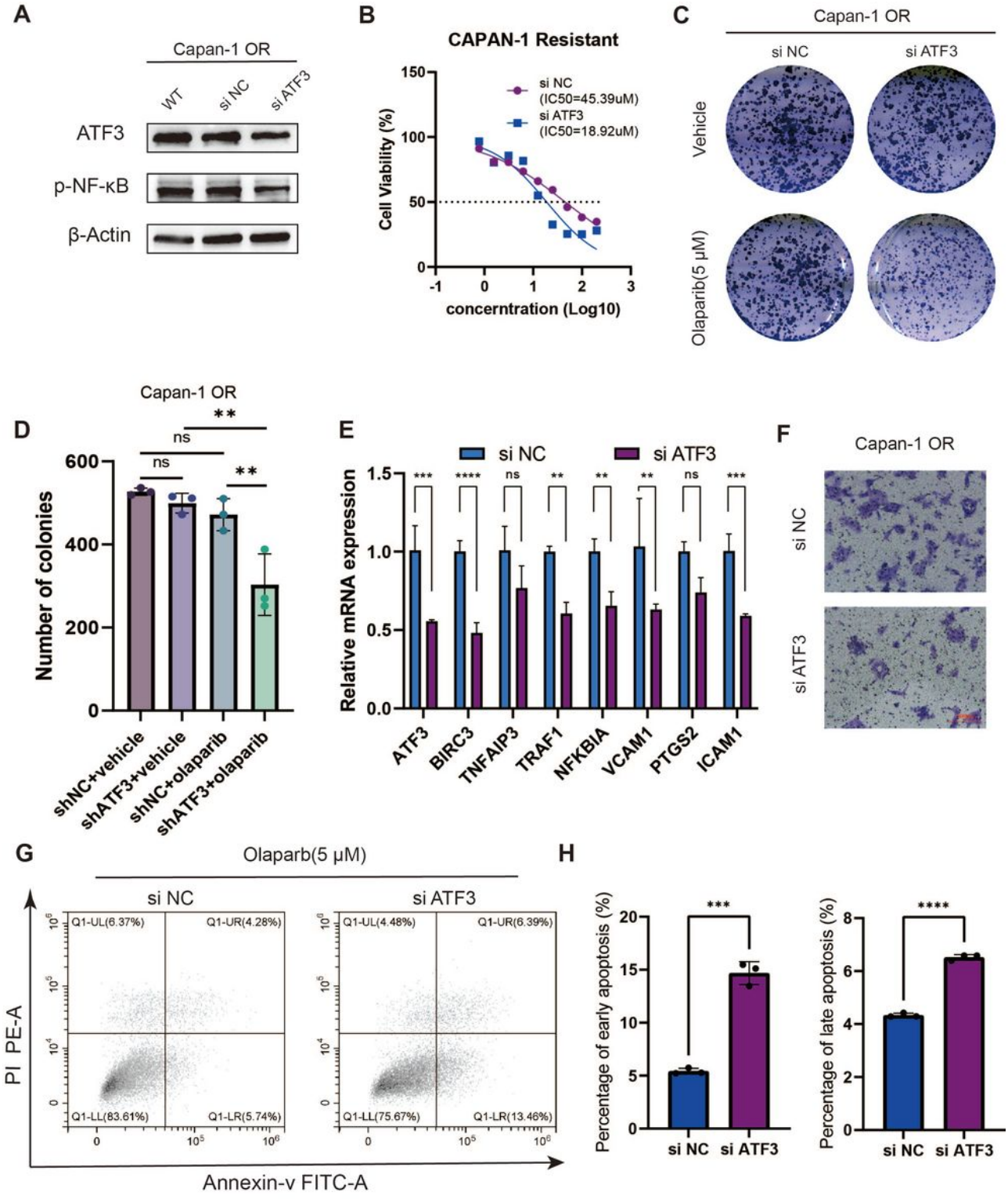

Figure 3

Effects of ATF3 silencing on NF-κB activity and resistance of OR cells to olaparib. (A) Western blot analysis of Capan-1-OR cells (siNC/siATF3) used to detect expression of ATF3, p65 and p-p65. (B) Cell viability evaluated using the CCK-8 assay following treatment of Capan-1-OR cells (siNC/siATF3) with different concentrations of olaparib. (C-D) Colony formation assays was used to test the impact of olaparib on the proliferative capacity of different cells. Cells were transfected with siRNA for 24 hours after 10 days of growth and then treated with olaparib or vehicle for 72 hours. (E) Real-time quantitative PCR analysis of mRNA expression for genes regulating the NF-κB signaling pathway in Capan-1-OR cells (siNC/siATF3). (F) Evaluation of invasiveness using a transwell assay. (G-H) Flow cytometric evaluation of apoptosis following treatment of Capan-1-OR cells (siNC/siATF3) with olaparib (5 μM) for 72 h (n=3). Data are expressed as mean ± SD; NS: not significant; $^{*}P < 0.05$; $^{**}P < 0.01$; $^{***}P < 0.001$; $^{****}P < 0.0001$.

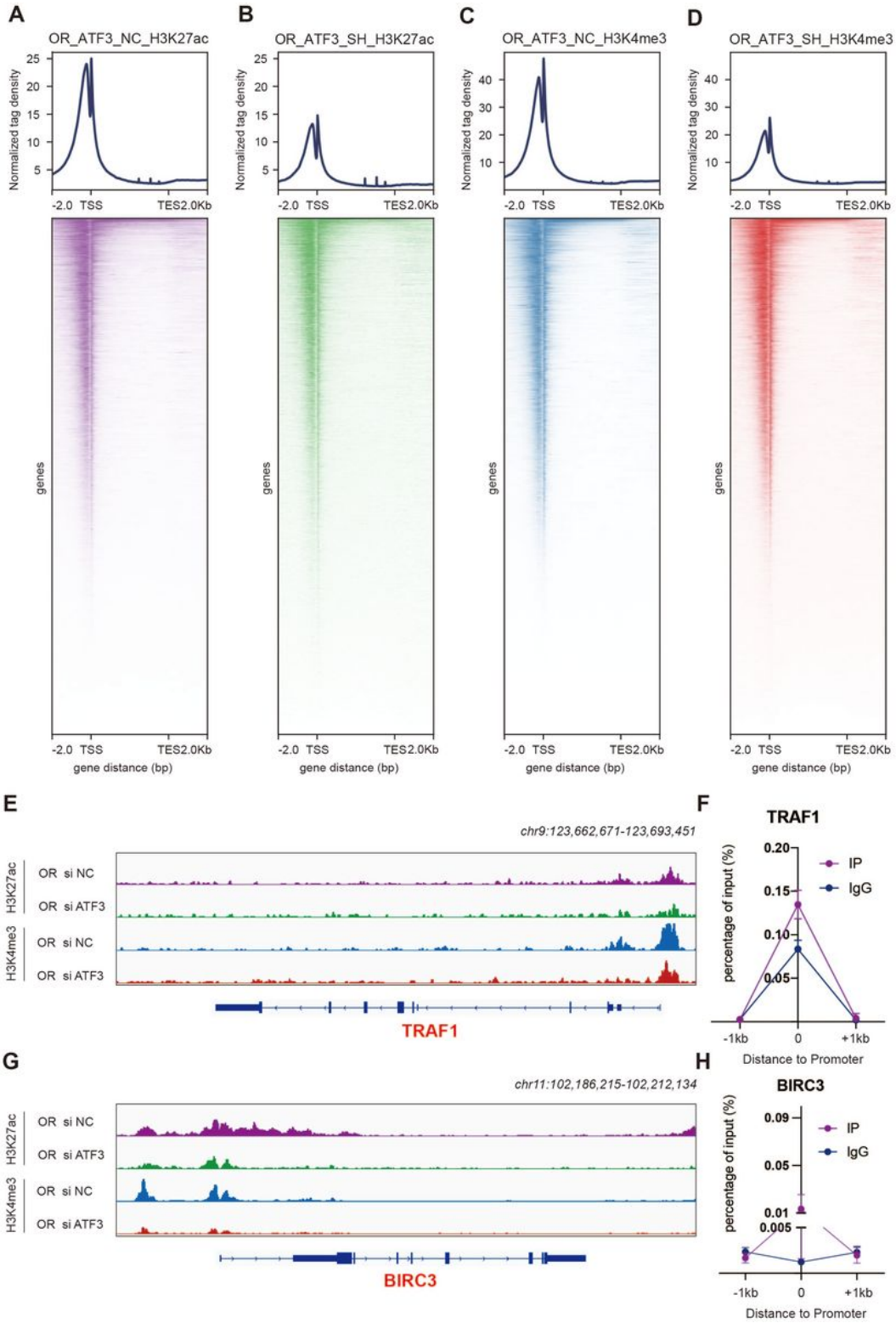

Figure 4

ATF3 binding to the promoter regions of essential regulatory genes in the NF-κB pathway. (A-D) Heatmap and signal density map for H3K27ac and H3K4me3 in Capan-1-OR cells (siNC/siATF3). (E, G) Genome browser tracks of ChIP-seq signals for genomic regions near TRAF1 and BIRC3. (F, H) Binding of ATF3 to the promoter regions of TRAF and BIRC3 in Capan-1-OR cells determined by chromatin immunoprecipitation-qPCR analysis.

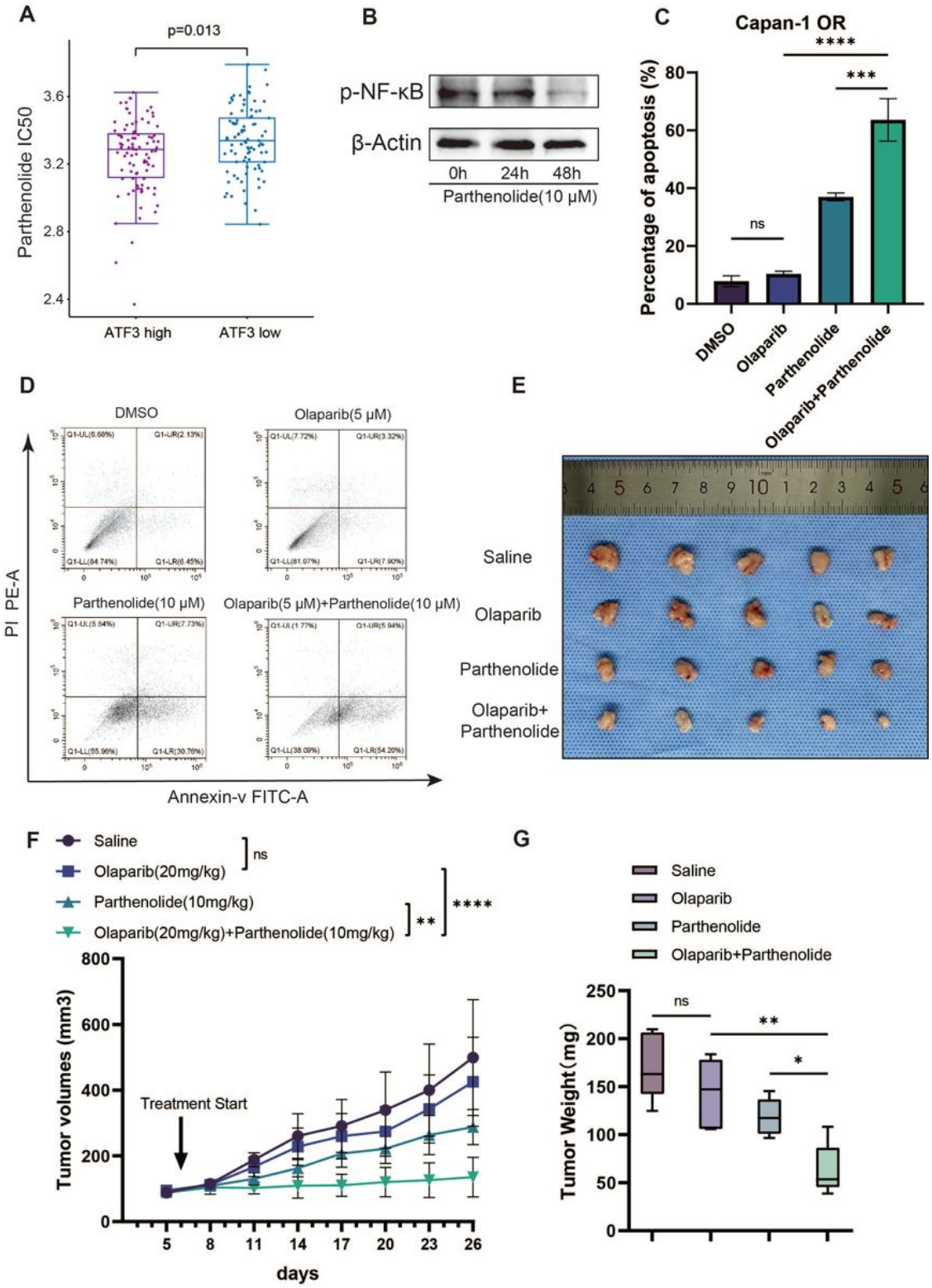

Figure 5

NF-κB inhibitor parthenolide reversal of PDAC resistance to olaparib in vivo and in vitro. (A) Correlation between ATF3 expression and the IC50 score of parthenolide. (B) Western blotting showed a time-dependent reduction of p-p65 levels by parthenolide. (C-D Flow cytometric evaluation of apoptosis following treatment of Capan-1 OR cells with olaparib (5 μM) and parthenolide (10 μM) alone or in combination for 72 h. Detection of apoptosis using flow cytometry and quantification of early or late

apoptosis rates (n=3). The differences among groups were analyzed by one-way ANOVA. (E) Construction of a subcutaneous tumor model in BALB/c nude using Capan-1 OR cells. Tumor-bearing mice were treated with saline, olaparib, parthenolide, or olaparib + parthenolide. Tumor volume was measured every three days following injection of cells, and the drug was administered from the sixth day. (E) The tumor volumes of different groups were measured with Vernier calipers. Two-way ANOVA was used to analyze the differences among groups. (F) Mice were executed at the end of the experiment, the tumors were removed and weighed. Results are presented as mean ± SD; NS: not significant; $^{*}P < 0.05$; $^{**}P < 0.01$; $^{***}P < 0.001$; $^{****}P < 0.0001$.

Supplementary Files

This is a list of supplementary files associated with this preprint. Click to download.

- FigureS1.jpg
- FigureS2.jpg
- SupplementaryTableS1.xlsx
- SupplementaryTableS2.xlsx
- SupplementaryTableS3.xlsx